JOURNAL OF MATERIALS SCIENCE 27 (1992) 4899–4908

# Predicting the tensile strength and creep–rupture behaviour of pultruded glass-reinforced polymer rods

L. FRANKE, H.-J. MEYER
*Institute of Physics and Materials in Civil Engineering, Technical University of Hamburg–Harburg, Eißendorfer Straße 42, 2100 Hamburg 90, Germany*

In pursuit of an optimization of the mechanical properties of glass-reinforced polymer (GRP) rods, a fracture mechanism is submitted which enables the description of the short-term strength and the creep strength behaviour. By means of short-term tension or relaxation tests on fibres, as well as compound tests for the determination of the interlaminar shear strength, the characteristic values are determined, which allow a prediction of the industrially produced GRP rods. This makes it possible to determine suitable glass and matrix materials in advance to find optimal rod conditions.

## 1. Introduction

Developments are currently being made in various places to use unidirectionally reinforced glass-reinforced polymer (GRP) rods as tension rods in civil engineering, both as prestressing elements in prestressed concrete constructions and as tension members in earth anchors [1]. In Fig. 1 we can see a pedestrian bridge produced with GRP tension elements. These elements are running freely under the bridge. Fig. 2 shows a cross-section through a prestressing element grouted with resin mortar used in a highway bridge in Düsseldorf. This bridge is prestressed with elements consisting of 19 bars. GRP tension rods have been in use for some time now for bracing masts and securing rocks.

In order to assess better the experimentally determined behaviour, and in view of the further development of GRP rods by specific selection of the components comprising the composite material, we shall introduce a method which allows reliable predictions of the short-term and creep-strength behaviour on the basis of simple tests with the components using a model for the fracture mechanism. The results of Rosen [2] and Overbeck [3] are used as basic data.

We will first introduce the fracture mechanism model of the unidirectional composite material for computing the mechanical short-term and creep–rupture behaviour. Experiments on glass-fibre bundles and tests for determining the interlaminar shear strength furnish the parameters required for predicting the mechanical short- and long-period properties of the rods. This procedure allows us to examine matrix and glass materials in advance, in order to produce rods with ideal properties.

*Figure 1* Bottom view of a pedestrian bridge in Berlin Marienfelde.

## 2. Fracture mechanism of rods under short-term tensile tests

Until now, estimations of the short-term rupture strength have used the failure models of Rosen [2] and Zweben [4]. In the "cumulative weakening model" of Rosen [2] from 1964, the strength of the fibre bundle is described using a Weibull distribution. This model also assumes that the fibres which tear before the GRP rod breaks, only fail to bear their share of the stress in the direct vicinity of the rupture. The lengths of fibre from a rupture point up to the point at which the fibres can take full load is described as the ineffective length. The GRP rod is regarded as a series of such layers consisting of glass-fibre segments in the form of chain links. The total load on the rod is assumed to be equally distributed over the cross-section of all unbroken fibres. This model leads to an excessively high estimation of rupture strength. The following text concentrates on further development of Rosen's [2] model, which is obviously realistic to a great extent. The description of the fracture mechanism finally

0022–2461 

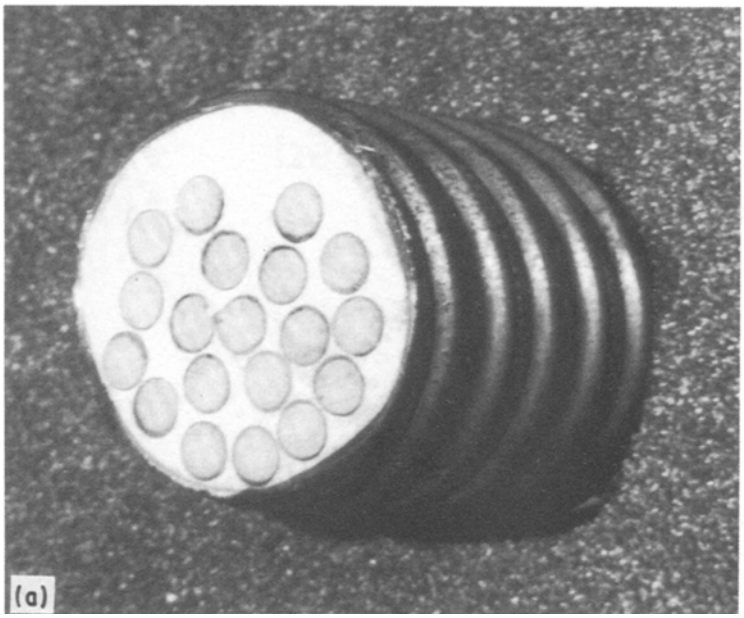



*Figure 2* (a) Cross-section through a highway bridge in Düsseldorf, and (b) detail of an anchoradge element.

allows both reliable prediction of the ultimate strength, and the creep strength behaviour.

## 2.1. Effective layer thickness, $l_s$

In accordance with the ideas of Rosen [2] it can be assumed that the fibre failure which occurs in a cross-section of a compound rod when the load is increased, will lead to an effective fibre length, $l$, at the breakage points, which can be defined as "elementary length, $l_s$", or to effective uncompounded fibre lengths or effective layer thicknesses of length, $l_s$. The effective layer thickness, $l_s$, can be imagined in accordance with Fig. 3. $l_s$ corresponds to the force introduction length at the ends of the fibre or at the breakage point of a fibre. A bundle of fibres of this length, $l_s$, thus has the mechanical properties of a GRP rod. If, realistically, we assume a constant compound tension distribution as a mean value of the practically triangular force introduction at the end of the fibre, depending on the individual fibre tension glass, the fibre diameter, $d$, and the composite strength, $\tau_{max}$, is

$$l_s(\varepsilon) = \frac{\varepsilon E d}{4\tau_{max}} \quad (1)$$

In GRP rods made of E-glass and an unsaturated polyester (UP) matrix, $l_s$ is about 0.5 mm [3]. To determine the layer thickness, the interlaminar shear strength must be known. It can be determined experimentally from manually produced composite material, e.g. by the ramp–stamp method (cf. Fig. 4).

The disc-shaped cuttings of compound material samples press stamps through the core. Fig. 4 shows the results of the tests with an epoxy resin matrix and the roving of type E16, comparing our own and an industrial production as a function of disc thickness. The compound strength to be used in the calculation is derived from Equation 2

$$\tau_{max} = \frac{\text{interlaminar shear strength}}{b} = \frac{F_{max}}{bDl\pi} \quad (2)$$

where $D$ is the stamp diameter in the shear test, $l$ the disc thickness of the sample, $b = 1.2$, a factor to account for the structurally conditioned roughness of the sheared-off shell surface. Table I gives the values for three selected roving types E8, E10 and E16.

## 2.2. Tensile strength of glass fibres and fibre bundles (rovings)

We have ascertained that to predict the behaviour of rod materials, the behaviour of the glass fibres must be known. Not all glass fibres manufactured under identical conditions have the same ultimate strength. The reason for this is the statistical distribution of faults in the fibres. In an unsorted quantity of glass fibres the individual fibre strength can be described by the distribution equation published by Weibull [5].

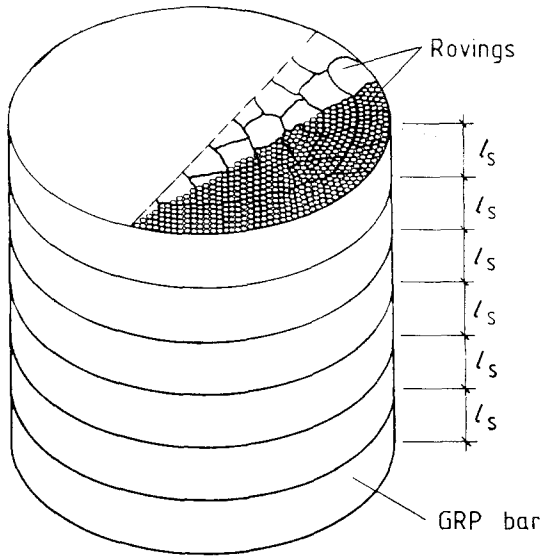


*Figure 3* Effective layer thickness, $l_s$.

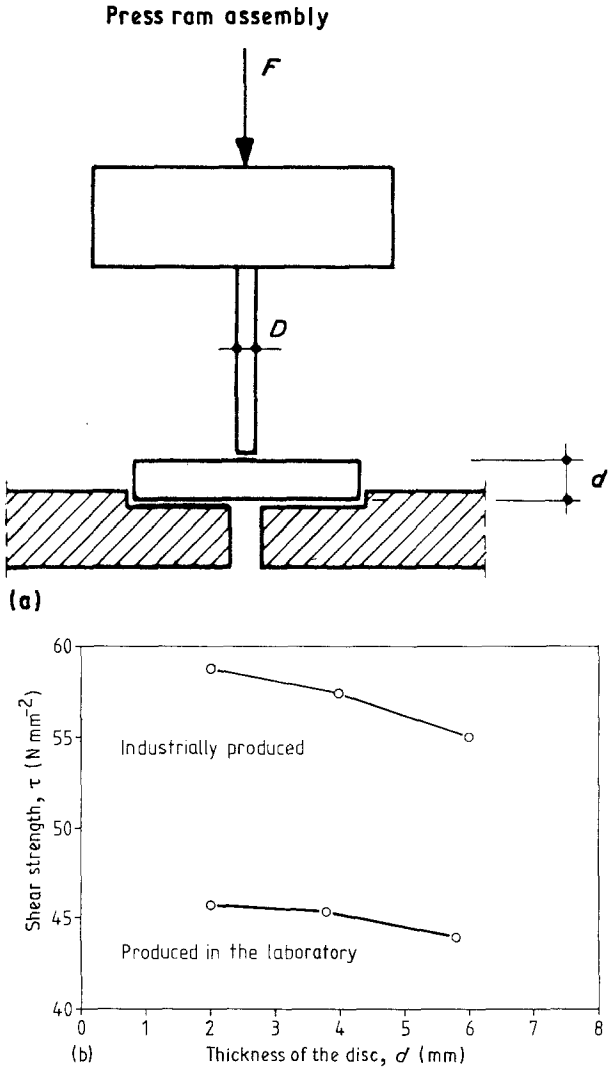


*Figure 4* (a) Stamp test set-up and (b) results of the experimentally determined interlaminar shear strength, τ, of roving type E16 in an epoxy resin matrix without accounting for the roughness of the shell surface.

The "simple" two-parameter Weibull distribution (cumulative frequency curve) suffices here

$$P(\beta) = 1 - \exp\left[-\left(\frac{\beta}{\beta_0}\right)^m\right] \qquad (3)$$

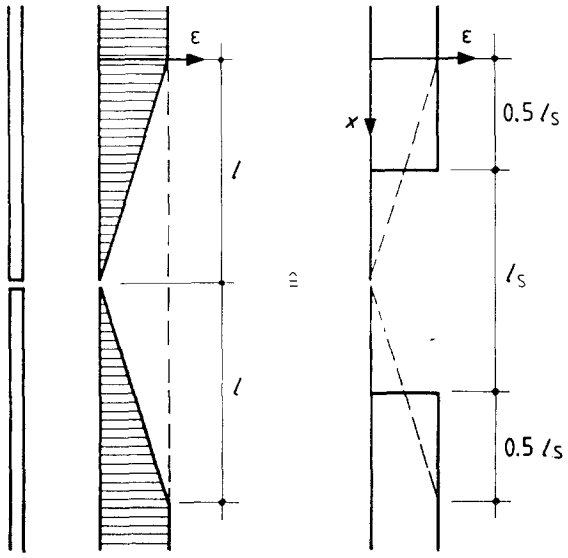


TABLE I Values for comparison

| Type of fibres | Resin | Tex (g km$^{-1}$) | Fibre diameter (μm) | Compound strength (N mm$^{-2}$) |
|---|---|---|---|---|
| E8 | UP | 2400 | 24.4 | 36 |
| E10 | EP | 2360 | 17 | 51 |
| E16 | EP | 2380 | 16 | 51.5 |

where β is the variable (e.g. strength or elongation at rupture of the individual fibres), $\beta_0$ is the Weibull parameter representing a kind of "mean value" and specifying the value of the variables (e.g. strength) which 63.2% of the fibres do not reach, and $m$ is the Weibull exponent, which provides a measure of the spread of variables, β.

Figs 5 and 6 show the influence of the exponent $m$ for a given $\beta_0$ or $\varepsilon_0 = \beta_0/E$.

Equation 3 applies for a constant fibre or sample length, $l_0$. This length was selected at $l = 300$ mm for reasons concerning the technicalities of the test. In order to use fibre length, $l_0$, to reach conclusions about other fibre lengths, we apply the "weakest link theory". Taking the failure and survival probability of a section into account (cf. [2, 6, 7]), for a roving of length $l$, where the strength distribution of the roving of length $l_0$ is known, we arrive at Equation 4.

$$P(\varepsilon) = 1 - \exp\left[-\left(\frac{l}{l_0}\right)\left(\frac{\varepsilon}{\varepsilon_0}\right)^m\right] \qquad (4)$$

In Equation 4, strength β has been replaced by elongation at rupture, ε, which is easily possible due to the linearity between elongation at rupture and tension in glass fibres. Fig. 7 shows the cumulative frequency distributions $P(\varepsilon)$ for various values of $l$.

The 63.2% elongation value, $\varepsilon_0$, changes with fibre length, $l$, as follows

$$\varepsilon_0^* = \varepsilon_0\left(\frac{l_0}{l}\right)^{1/m} \qquad (5)$$

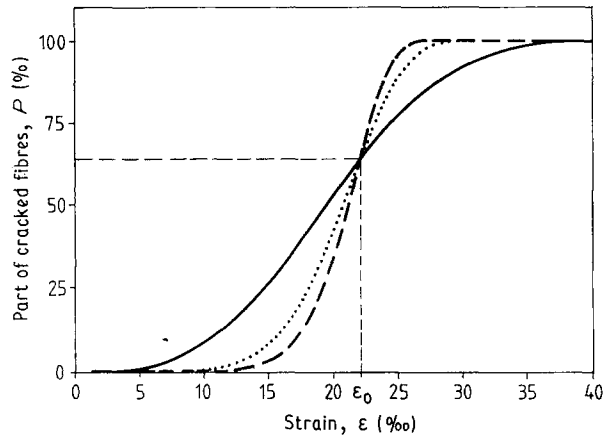


*Figure 5* Cumulative frequency of the share of torn fibres as a function of Weibull exponent, $m$: (———) 3, ( • • • ) 6.24, (– – –) 9.

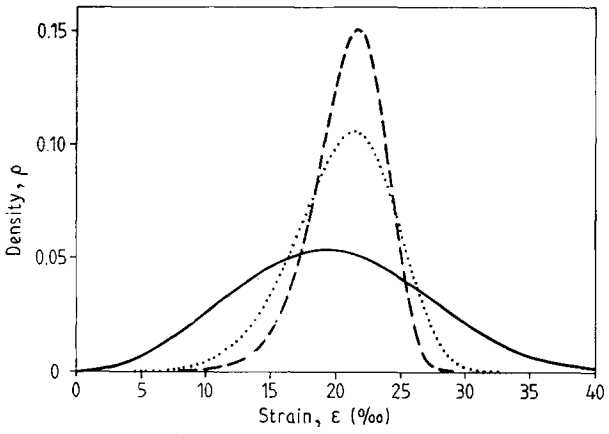


*Figure 6* Distribution function for Fig. 3. $m$: (———) 3, ( • • • ) 6.24, (– – –) 9.

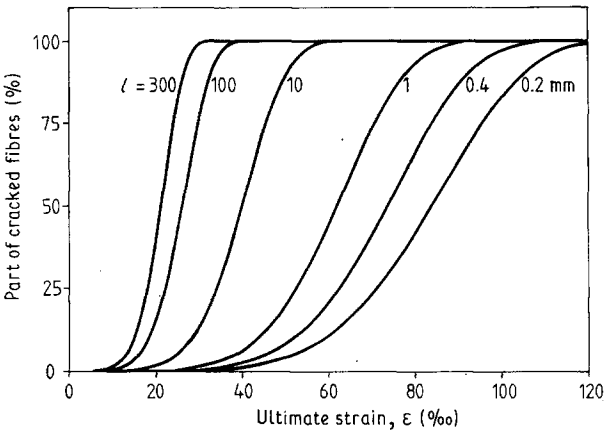


*Figure 7* Fracture behaviour (cumulative frequency curves) as a function of roving length.

Tensile tests are necessary to determine experimentally the distribution of strength and elongation at rupture for a given fibre type. As it is very difficult to test the individual fibres, the more practical method is used for determining strength distribution by testing whole bundles of fibres, which we will call rovings. A roving consists of 2000–4000 fibres, depending on the type of fibre. The roving samples are suitably anchored at the ends, leaving a free length of about 300 mm. This anchoring is used to clamp the sample in a tensile testing machine. In a short-term tensile test recording the force/elongation diagram, the percentage of torn fibres is determined by Equation 6, at an elongation speed of 1% $min^{-1}$.

$$P(\varepsilon) = 1 - \frac{F(\varepsilon)}{F_T(\varepsilon)} \tag{6}$$

where $F_T(\varepsilon)$ is the force/elongation curve without the share of torn fibres (initial slope) and $F(\varepsilon)$ is the measured curve

$$F_T(\varepsilon) = E_{glass}\,\varepsilon \cdot A_R \tag{7}$$

The cumulative frequency distribution, $P(\varepsilon)$, we are looking for must now correspond to the relative sum in the elongation-controlled tensile test (Equation 4). Equations 6, 7 and 4 provide the required equation for the curve in the force/elongation diagram (Fig. 8)

$$F(\varepsilon) = \varepsilon E A_R \exp\left[-\left(\frac{l}{l_0}\right)\left(\frac{\varepsilon}{\varepsilon_0}\right)^m\right] \tag{8}$$

To determine the Weibull parameter on the basis of tensile tests, it is necessary to transform Equation 8 into a graph with the axes $\ln \varepsilon$ and $\ln \ln[1/(1-P)]$, because the distribution equation appears as a straight line here. It is possible to estimate this straight line with "linear regression". The slope of the line determines the parameter $m$, and the crossing point with the $\ln \varepsilon$ axis determines $\varepsilon_0$. Fig. 9 shows the part of cracked fibres depending on the elongation, $\varepsilon$, and Fig. 10 explains the above mentioned transformation and the determination of the Weibull parameter.

To determine the ultimate strength of the GRP rods it is necessary to know the maximum load of a roving. This we obtain by deriving Equation 8 and calculating the zero point of the derived function. With this procedure we obtain the ultimate elongation. Equation 9 shows the result of this elongation, $\varepsilon_u$, with respect to the influence of the length

$$\varepsilon_u = \left(\frac{l_0}{l}\right)^{1/m}\left(\frac{1}{m}\right)^{1/m}\varepsilon_0 \tag{9}$$

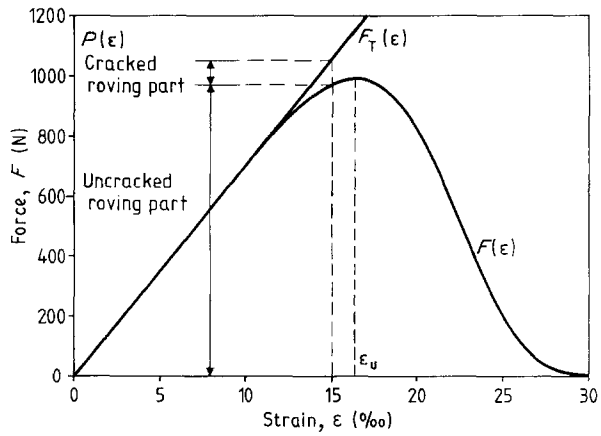


*Figure 8* Force/elongation diagram of a roving test.

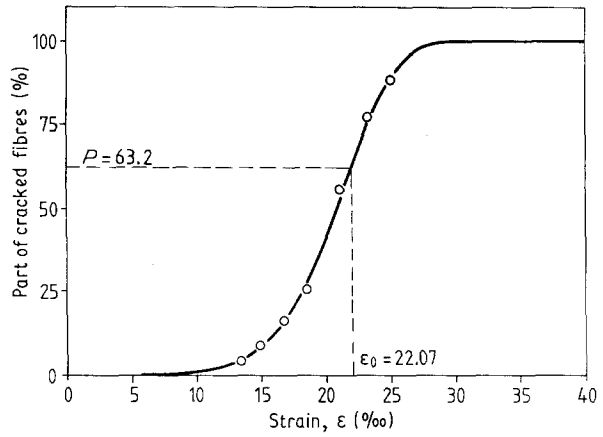


*Figure 9* Part of the cracked fibres (E-glass, Series E10): (○) mean measured value, (——) Weibull cumulative frequency curve.

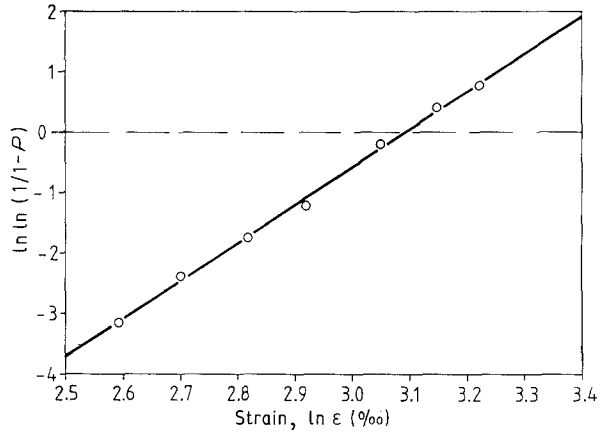


*Figure 10* Transformation into Weibull paper: (○) mean measured value, (——) straight line from regression analysis.

The percentage of fibres torn at the moment of fracture is derived by inserting Equation 9 into Equation 4

$$P(\varepsilon_u) = 1 - \exp\left(-\frac{1}{m}\right) \quad (10)$$

We can see from this that the Weibull exponent, $m$, determines the percentage of torn fibres at failure. The smaller the exponent $m$, the larger the share of torn fibres at breakage. The sample length has no influence on this percentage. For the values of $m$ used as examples in Figs 5 and 6, Equation 10 produces the fibre percentages belonging to the maximum load of the corresponding rovings at 28.4%, 14.8% and 10.5%.

## 2.3. Strength of a GRP rod from one roving

The elongation, $\varepsilon_u$, associated with the maximum accepted tensile force of a nacked roving, and the associated percentage of torn fibres, are provided by Equations 9 and 10. After impregnating with resin and hardening, this type of roving acquires rod properties. The associated force/elongation line, $F(\varepsilon)$, is then given by Equation 8, whereby it should be noted that the effective layer thickness, $l_s$, to be inserted for $l$ is itself dependent on the rod force or elongation

$$l = l_s = \varepsilon\left(\frac{E_{glass}\, d}{4\tau_{max}}\right) = \varepsilon K_s \quad (11)$$

$$F(\varepsilon) = A_R\, E_{glass}\, \varepsilon \exp\left(-\frac{k_s\, \varepsilon^{m+1}}{l_0\, \varepsilon_0^m}\right) \quad (12)$$

The maximum accepted force of the roving rod is produced by Equation 12 after inserting $\varepsilon_u$ from Equation 9 and using Equation 11, and is

$$F_{max} = E_{glass}\, A_R\, \varepsilon_0^{m/(m+1)} \left(\frac{l_0}{K_s}\right)^{1/(m+1)} \times \left(\frac{1}{m}\right)^{1/(m+1)} e^{-1/m} \quad (13)$$

Impregnating the fibres with a resin matrix increases the elongation at rupture and the strength of the roving. For example, the mean fracture load of the nacked roving E10 (300 mm sample length) is 1025 N. The characteristic Weibull parameters of the roving are $\varepsilon_0 = 2.207\%$, $m = 6.24$. After impregnating with resin ($\tau_{max} = 51\ N\,mm^{-2}$) we obtain from Equation 13 a calculated roving rod fracture load of 2.33 kN; the average actually measured was 2.23 kN.

The discrepancy between calculation and experiment is only 4%. The effect of the resin matrix on the force/elongation line of a roving is shown in Fig. 11.

## 2.4. Prediction of the mechanical short-term properties of a GRP rod consisting of several rovings

Unidirectionally reinforced GRP rods usually consist of a number of rovings; the 7.5 mm thick Polystal rods (Bayer AG), for example, consist of $z = 32$ rovings. If we now test a roving type using, say, 10 roving samples with 300 mm free length, we obtain spreading tension/elongation lines with the basic curve corresponding to Fig. 11 or Equation 8. By grouping all rovings to form an "overall roving" and dividing by the number of rovings, we obtain what is called the

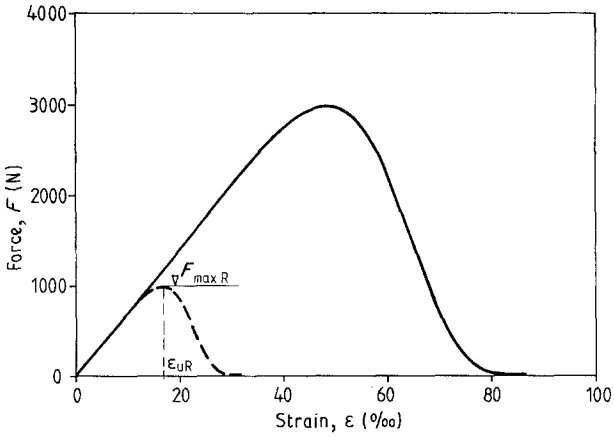


*Figure 11* Comparison of the force/elongation lines of (– –) a nacked and (——) an embedded roving E10.

"mean value roving", which would seem suitable for predicting the behaviour of the rods produced from it. However, if we calculate the rod ultimate force, assuming that it is produced by $z$ mean value rovings, we will usually arrive at ultimate loads which are far too high. This, in turn, is illustrated by roving type E10: for the mean value roving of fibre type E10, $\varepsilon_0 = 2.207\%$, $m = 6.24$. Also $\tau_{max} = 51\ N\,mm^{-2}$. From Equation 13 we obtain, at $z = 32$, the rod fracture force of 91.6 kN. The associated calculated elongation at rupture, $\varepsilon_u$, is calculated from Equation 9 if

$$l = l_{s(\varepsilon_u)} = K_s^{m/(m+1)} l_0^{1/(m+1)} \left(\frac{1}{m}\right)^{1/m} \varepsilon_0^{m/(m+1)} \quad (14)$$

is used there. It is 4.84%. By contrast, the measured ultimate fracture force is only 70.4 kN and the associated elongation 3.3%. Fig. 12 shows a typical force/elongation line for this type of rod.

A closer examination of the fracture behaviour and the measured fracture characteristics now leads us to the conclusion that a rod made from a larger number, $z$, of rovings will fail when the weakest rovings fails, delaminating the entire rod. Fig. 13 shows part of a cross-section through an industrially produced GRP rod. Although the rods are produced according to the pultrusion method, the individual rovings are slightly visible.

The decisive roving is thus produced by statistical evaluation of the tensile tests on each roving type, and is described here as a "decisive roving" or "fractile roving". The associated Weibull parameters are $\varepsilon_{0,f}$ and $m_f$. Fig. 14 shows the force/elongation lines determined in the experiment for the mean value roving and the fractile roving of fibre type E10 ($l_0 = 300$ mm), with the $F(\varepsilon)$ lines, referred to $l_s$, which were calculated from those rovings and which are decisive in the rod. The actual ultimate force of a GRP rod in the short-term tensile test is thus obtained from

$$F_{max(rod)} = cz F_{max}, \quad (15)$$

if the Weibull parameters $\varepsilon_{0f}$ and $m_f$ of the fractile roving are used in $F_{max}$ from Equation 13. The factor $c$ (as a rule $c \approx 0.96$) is an experimentally obtained factor and accounts to the influence of the edge fibres which are not fully encased in resin. The associated elongation at failure is at least $\varepsilon_{Br}$; it is obtained from Equation 12 for $F(\varepsilon) = F_{max(rod)}$ by resolving $\varepsilon$ and inserting the Weibull parameters of the mean value roving.

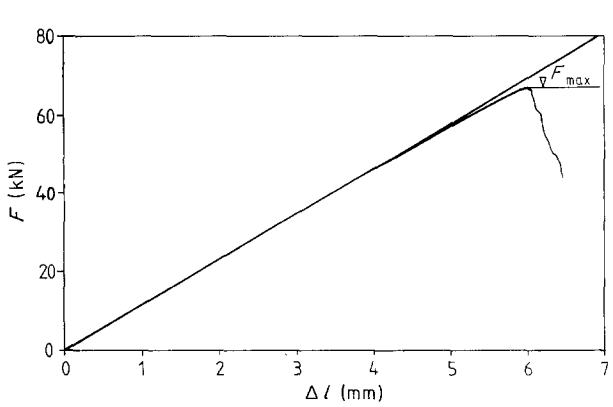


*Figure 12* Force/elongation diagram of a GRP rod = 7.5 mm, glass content ~ 80% by weight.

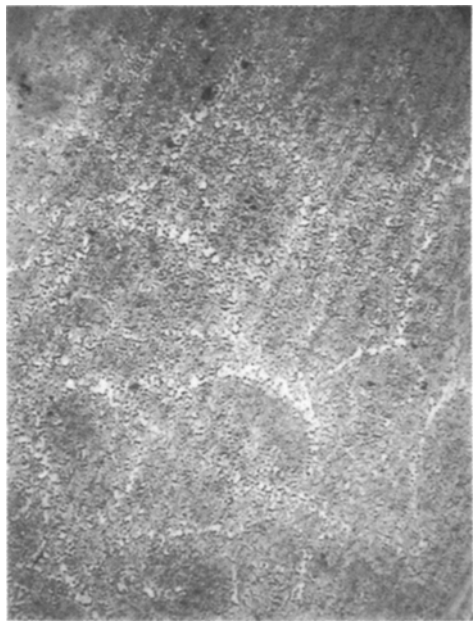

*Figure 13* Cross-section through an industrially produced GRP bar.

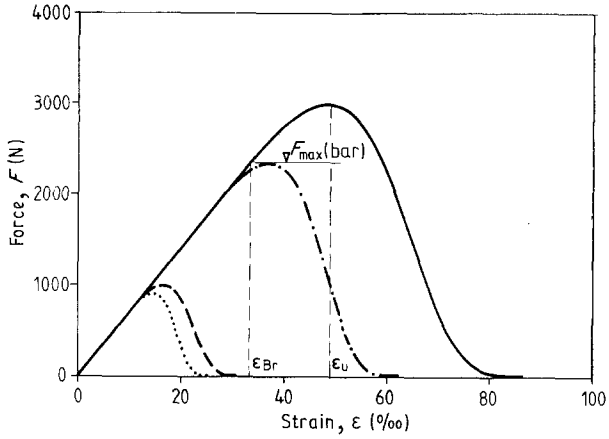


*Figure 14* Force/elongation lines of nacked and embedded rovings of fibre type E10. (——) Mean roving $l_s$ (bar), (—·—) fractile roving, $l_s$ (bar), E10. (– – –) mean roving $l = 300$ mm, ( ••• ) fractile roving, $l = 300$ mm.

Table II shows the rod fracture loads for fibre types E8, E10 and E16 predicted using the method described above, in comparison with the measured ultimate loads of the rod. We notice that the discrepancies between prediction and experiment are less than 5%.

## 2.5. Influence of compound strength, $\tau_{max}$, on rod fracture loads

In assessing the mechanical properties of a compound rod consisting of $z$ rovings it is of interest to know the influence of the quality of the compound between fibres and resin, as well as any change in the elementary length, $l_s$. Fig. 15 below shows the change in length, $l_{s(Br)}$ and in fracture force, $F_{Br}$, of the rod material when using fibre material E10. By varying the Weibull parameter, $m$, we can clearly see the influence of the glass-fibre strength spread on the compound properties ($\tau_{max}$) and on the rod strength. The larger is

TABLE II Determined Weibull parameters and the calculated time-dependent strength values compared with the test results

| Type of fibres | Resin | Weibull parameter | | | | Rods to be composed of 32 rovings | | | | |
|---|---|---|---|---|---|---|---|---|---|---|
| | | Mean roving | | Fractile roving | | | Predicted | | Measured values | |
| | | $\varepsilon_0$ (‰) | $m$ | $\varepsilon_f$ (‰) | $m_f$ | $l_s(\varepsilon_{Br})$ | $F_{Br}$ (kN) | $\varepsilon_{Br}$ (‰) | $F_{Br}$ (kN) | $\varepsilon_{Br}$ (‰) |
| E8 | UP | 17.7 | 4.42 | 17.0 | 6.2 | 0.4 | 66.8 | 31 | 68.7 | 31 |
| E10 | EP | 22.07 | 6.24 | 19.0 | 7.5 | 0.21 | 71.5 | 33 | 70.4 | 32.8 |
| E16 | EP | 22.3 | 9.46 | 21.5 | 9.0 | 0.18 | 75.3 | 36.5 | 78.2 | 36.2 |

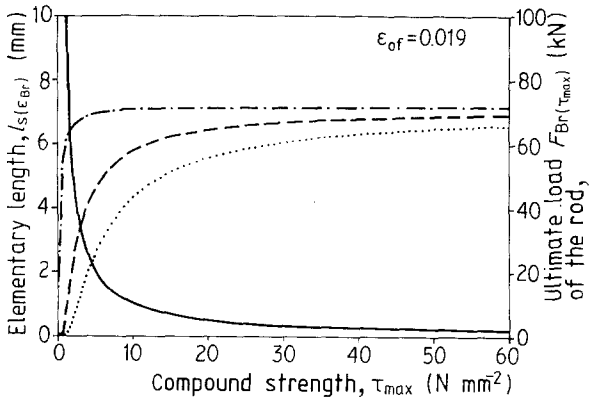


*Figure 15* Dependence of rod fracture force and elementary length, $l_s$, on the compound strength for various Weibull parameters, $m$: (——) 3, (– – –) 7.5, ( ••• ) 9.

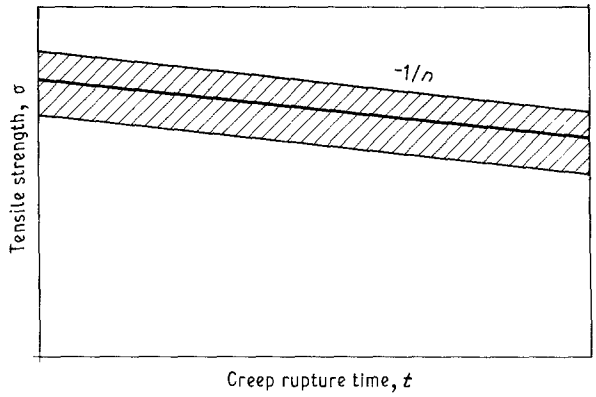


*Figure 16* Long-period behaviour of individual fibres under normal climatic conditions (spread range as given by Weibull statistics).

parameter $m$, the greater is the influence of $\tau_{max}$ on rod strength.

## 3. Long-period behaviour

After the description of the short-term behaviour of the GRP rod, we shall examine the creep–rupture behaviour in more detail. The elaborations indicate the extent to which the creep–rupture behaviour of the rods depends on the mechanical properties of the components and on the compounding between the fibres and the resin, and illustrate the measures with which this behaviour can be optimized.

### 3.1. Long-period behaviour of glass fibres and rovings

Predicting the rod behaviour under constant load requires that we know the creep–rupture behaviour of the glass fibres. In the literature we find reports of creep–rupture tests on individual fibres, in particular optical fibres, and on solid glass (cf. [8–12]). The results of these tests show that the creep–rupture behaviour of the glass samples or fibre samples of a parent population can be characterized by a straight line on double logarithmic scale in accordance with Fig. 16. For glass fibres, $n$ is by order of magnitude equal to 40 (cf. [3, 12, 13]). The long-period behaviour of individual fibres is therefore described by the relation

$$t(\sigma) = \frac{1}{B_1 \sigma^n} \tag{16}$$

During the period leading up to the failure, the decisive faults or cracks in the individual fibres grow at a defined rate of crack propagation until they reach the critical size. The rate of crack propagation at constant fibre tension is

$$\frac{da}{dn} = A_1 k_1^n(t) \tag{17}$$

$A_1$ is a material coefficient dependent on the initial crack length, $a_1$, and the ambient conditions, $k_1$ is the tension intensity in accordance with the $K_c$- concept of fracture mechanics, and $n$ is the exponent in accordance with Fig. 16 or Equation 17. The endurance of the $i$ fibres of a collective (which varies in spite of constant tension) or the endurance spread of the fibres, is caused by different sizes of faults or initial crack lengths, $a_1$, when the stress commences. The influence of the initial crack length or strength spread can be accounted for in the material coefficient, $B_1$. According to Franke [14], we obtain the relation of the endurance values between fibres of different strengths from the following

$$\frac{B_i}{B_1} = \left(\frac{a_i}{a_1}\right)^{(n-2)/2} \tag{18}$$

Furthermore, according to the $K_c$ concept of fracture mechanics, the following relation exists between the fault sizes, $a_i$, of the fibres and the fibre strengths

$$\left(\frac{a_i}{a_1}\right)^{1/2} \frac{\beta_i}{\beta_1} = 1 \tag{19}$$

From Equations 18 and 19 we obtain the connection between the fibre strengths and the material

coefficients, $B_1$, from Equation 16 at

$$\frac{B_i}{B_1} = \left(\frac{\beta_1}{\beta_i}\right)^{n-2} \tag{20}$$

The endurance of samples or fibres of the same kind but of different strengths, under the same tensile stress, $\sigma$ = constant, thus relates as

$$\frac{t_i}{t_1} = \left(\frac{\beta_i}{\beta_1}\right)^{n-2} \tag{21}$$

This relationship is illustrated in Fig. 17.

If a sample collective or fibre bundle of length $l$ has the following strength distribution (cumulative frequency curve), e.g. according to Weibull with the Weibull parameters $\varepsilon_0$ and $m$ (cf. Equation 3)

$$P(\beta_i) = 1 - \exp\left[-\left(\frac{\beta_i}{\beta_0}\right)^m\right] \tag{22}$$

creep–rupture tests on the individual fibres of the roving will produce the distribution of the associated endurance values, $t_i$ (cumulative frequency curve) on the tension level $\sigma$ is constant, using Equation 21, from the following relation

$$P(t_i) = 1 - \exp\left[-\left(\frac{t_i}{t_0}\right)^k\right] \tag{23a}$$

with

$$k = \frac{m}{n-2} \tag{23b}$$

as the exponent for the spread of the endurance values. The reference value of the endurance (63.2% value) changes as a function of the effective fibre length, $l$, in comparison with the reference length, $l_0$, as

$$t_{0,l} = \left(\frac{l_0}{l}\right)^{1/k} t_{0,l_0} \tag{24}$$

In many applications the question of spread ranges of the endurance of material samples or stressed components at a given load level is relevant. We can deduce from the relationships above that there is a direct connection between the spread of endurance values $t_i$ referred to the characteristic $t_0$ and the spread of the corresponding short-term strength values $\beta_i$ and $\beta_0$ (see Equation 25)

$$t_i = \left(\frac{\beta_i}{\beta_0}\right)^{n-2} t_0 \tag{25}$$

If, for example, the 5% fractile of the fibre strengths determines the mean strength value to 90%, a 5% fractile value of the endurance values can be expected, which is $90\%^{n-2}$ of the mean value. At a value of $n = 38$, realistic for glass fibres, we thus obtain the 5% fractile of the endurance values at approximately 2% of the mean value. The practical determination of $k$ or $n$ of a fibre type is done by means of tests at constant elongation (relaxation tests) on the whole roving, with the result that in spite of the time-dependent tearing of individual fibres, the tension of the fibres remains constant. In this type of test with initial load $F_0$, we obtain a curve as shown in Fig. 18. $F_0$ is selected using a $\sigma$–$\varepsilon$ line in such a way that none, or a negligibly small number, of the fibres tear under the initial load. The curve is produced by the following relation

$$P(t) = 1 - \frac{F(t)}{F_0} = 1 - \exp\left[-\left(\frac{t}{t_0}\right)^k\right] \tag{26}$$

or, in view of the practical evaluation at endurance values $< t_0$

$$\frac{F(t)}{F_0} = \exp\left[-\left(\frac{t}{t_0}\right)^k\right]. \tag{27}$$

The value $k$ being determined is produced by this as a slope of the logarithmic function (Equation 26)

$$\lg\left\{\ln\left[\frac{F(t_1)}{F_0}\right] - \ln\left[\frac{F(t_2)}{F_0}\right]\right\} = k(\lg t_1 - \lg t_2) \tag{28}$$

$n$ is obtained with $k$ from Equation 23b after inserting the Weibull parameter $m$ from the familiar strength distribution. Fig. 19 shows the relaxation curves measured on the rovings of the E10 series. The derived values $k$ and $n$ are taken from Table II.

## 3.2. Creep–strength behaviour of GRP rods

### *3.2.1. Deformation under constant load*

The deformation of pultruded glass fibre rods under constant stress was discussed previously [15]. It was

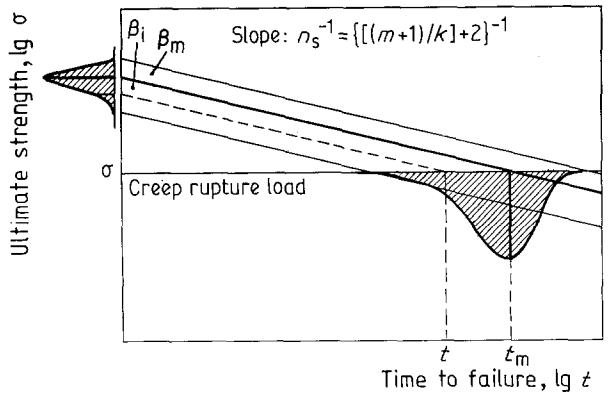


*Figure 17* Relationship of spread from the short-term tests and creep–rupture tests of glass fibres. $\beta_m$ is the mean value of ultimate strength, $t_m$ is the mean value of time to failure.

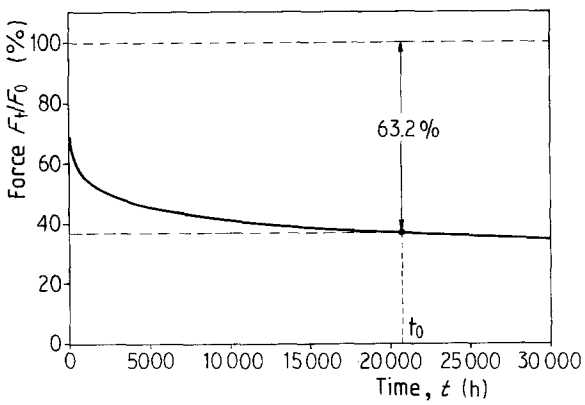


*Figure 18* Long-period behaviour of a roving at constant elongation ($F_0$ = initial load).

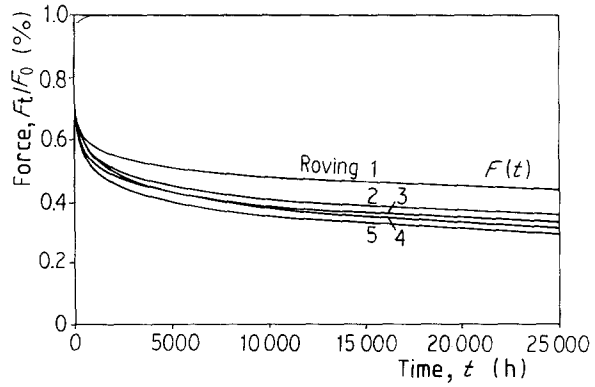


*Figure 19* Relaxation curves of the E10 roving.

shown that the glass fibres do not manifest any creep at normal temperatures. Only the relatively slight share of the load introduced at the onset of stressing into the resin matrix in accordance with its proportional rigidity is transferred in the course of time from the resin to the glass component as a result of relaxation, so that a slight increase in elongation is registered, which fades fast but can still be described as creeping. However, this increase is only about 3% of the initial elongation and it can therefore be neglected as a rule.

### 3.2.2. Endurance values at constant load

The creep–strength behaviour of the compound rods can be predicted on the basis of the creep–strength behaviour of the rovings if the effective layer length, $l_s$ is introduced as the decisive fibre length. $l_s$ corresponds to the force introduction length at the ends of fibres or at a fibre breakage point. As changes in tension and elongation amounting to only about 3% of the initial value occur up to shortly before the maximum endurance in a creep–rupture test under constant load, a constant elongation state can be assumed for the following considerations. Compared with the fracture state in the short-term test, the GRP rod has a shorter decisive fibre length, $l_s$, under working tension

$$l_s(t, \sigma) = l_s(\varepsilon_{Br}) \frac{\sigma}{\sigma_{Br}} [1 + \varphi(t)] \qquad (29)$$

where $\sigma$ is the rod tension as long-period stress, $\sigma_{Br}$ the ultimate strength of the rod, $l_s(\varepsilon_{Br}) = l_s$ at breakage in the short-term test, and $\varphi(t)$ is the coefficient with which a time-dependent increase of $l_s$ can be accounted for.

The endurance of the rod now corresponds to that of a corresponding roving with the short effective length, $l_s(t, \sigma)$, as in Equation 29. It is obtained by the following means. The endurance of a roving of length $l_0$ at constant elongation or tension of the individual fibres until endurance, $t_0$, of the fibres is reached (failure of 63.2%) is, according to Equation 16

$$t_{0,l_0}(\sigma_i) = \frac{1}{B_1 \sigma_i^n} \qquad (30)$$

Referred to this endurance, a roving of the (shorter) length $l_s$ has the following endurance (cf. Equation 22)

$$t_{0,l_0}(\sigma) = t_{0,l_0} \left[ \frac{l_0}{l_s(t, \sigma)} \right]^{1/k}. \qquad (31)$$

After introducing Equation 31 into Equation 30 and accounting for Equation 29, we obtain the expression for the required endurance of the rods (as the endurance of a short roving of length $l_s(t, \sigma)$) at

$$t_0(\sigma) = C_1 \left[ \frac{1}{B_1 \sigma^{(n+1/k)}} \right] \qquad (32)$$

with

$$C_1 = \left[ \frac{l_0 \sigma_{Br}}{l_s(\varepsilon_{Br})} \right]^{1/k} \left[ \frac{1}{1 + \varphi(t)} \right]^{1/k}$$

A comparison with Equation 16 shows that this is a straight line on double logarithmic scale with the slope

$$-\frac{1}{n_s} = -\frac{1}{n + (1/k)} \qquad (33)$$

as long as no time-dependent change of $l_s$ takes place, i.e. $\varphi(t) = 0$. This means that the endurance straight line of the rods is flatter than that of the roving component. Fig. 20 shows a comparison of the slopes of the roving and the rod.

The characteristics determined on the basis of or derived from the comparatively short creep–rupture tests on bare rovings, and a comparison of the data which have, in the meantime, been measured from compound rods, are shown in Table II. Fig. 21 shows the long-period straight line measured on the GRP rod of series E10 or calculated from the test values by linear regression.

An assessment of the above results indicates that surprisingly good predictions can be made about the creep–rupture behaviour of the unidirectionally reinforced GRP material with the help of the method described above. The test results show that under the given conditions (normal climatic conditions) no significant changes in the compound properties or the lengths $l_s$ could be registered.

The creep–rupture tests were conducted on specially constructed test stands. Spring packages were used to retain constant force. In order to compensate the (albeit slight) force reduction caused by the creeping of the sample, the force was checked in logarithmic time intervals and corrected as needed.

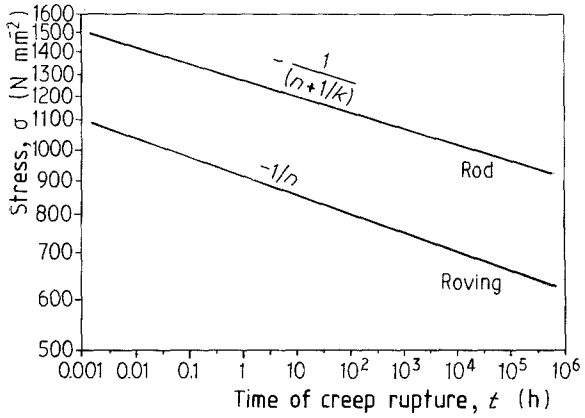


*Figure 20* Comparison of creep–rupture straight line of a roving and the rod made from it (series 10).

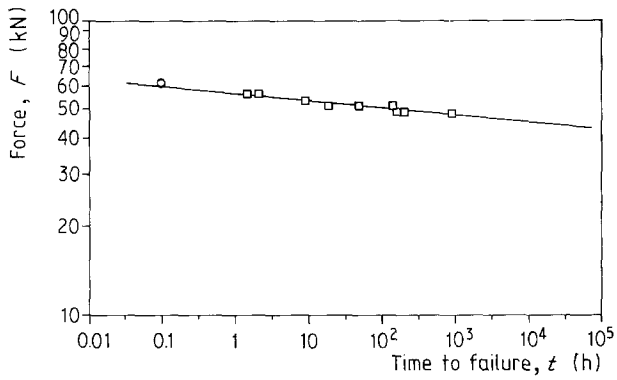


*Figure 21* Results of the (□) creep–rupture tests on series E10 material and of (○) two short-term tensile tests applied at $t = 0.1$ h.

If use of the results of the short-term tests conducted at a constant rate of load increase is to be included for setting up the long-period function, this can be done as follows. The short-term tensile test results are applied by using the accumulation rule for creep rupture stress (cf. [1]), as shown in Equation 34

$$\sum_{i=1}^{j} \frac{\Delta t_i}{T_b(\sigma_i)} = 1 \quad \text{breakage conditions} \tag{34}$$

$T_b(\sigma_i)$ is the time which leads to failure for a certain constant tension, $\Delta t_i$ is the time over which this tension is applied. The endurance of the GRP rods for a certain tension is calculated (cf. Equation 30) as follows

$$T_b = \left(\frac{1}{D_1 \sigma^{n_s}}\right) \tag{35}$$

where $D_1$ is the material coefficient $(1/\sigma_0^{n_s})$. $\sigma_0$ is the tension for an endurance of 1 h, i.e. $\lg t_0 = 0$. In accordance with the damage accumulation rule, when converting from one level 1 to another 2, the following consequently also applies

$$\frac{t_1}{t_2} = \left(\frac{\sigma_2}{\sigma_1}\right)^{n_s} \tag{36}$$

By varying $\sigma_2$ with progressing time it is possible to sum over all according time intervals, $\Delta t_i$. After separating $t_1$ we obtain Equation 37.

$$T_b = \sum_i \left(\frac{\sigma_i}{\sigma_1}\right)^{n_s} \Delta t_i \tag{37}$$

Choosing a linear increase of the force

$$\sigma(t) = at$$

and transforming the sum into an integral we obtain Equation 38

$$t_1 = \frac{1}{\sigma_1^{n_s}} \int_0^{t_b} \sigma(t)^{n_s} \, dt = \frac{1}{\sigma_1^{n_s}} \int_0^{t_b} a^{n_s} t^{n_s} \, dt \tag{38}$$

with the solution

$$t_1 = \frac{a^{n_s}}{\sigma_1^{n_s}} \frac{t_1^{n_s+1}}{n_s + 1} \tag{39}$$

If the short-term test is to be applied at an equivalent creep rupture value of $t = 0.1$ h, Equation 39 can be inserted into Equation 36 and for $t_2 = 0.1$. We then obtain the equivalent creep–rupture load or tension calculated from the short-term strength at

$$\sigma_2(t = 0,1 \text{ h}) = \frac{1}{(0,1a)^{1/n_s}} \times \left(\frac{1}{n_s + 1}\right)^{1/n_s} \sigma_1^{(n_s+1)/n_s} \tag{40}$$

## 4. Conclusion

The present work describes the computation of the fracture mechanism of GRP rods for predicting the mechanical properties in short-term tests and for predicting long-period behaviour. Using the results of experimental tests, it is shown that on the basis of Weibull statistics in evaluating the strength of the glass fibres or rovings and the compound strength of the glass fibre/resin matrix, a reliable prediction of the tension and elongation behaviour in short-term tests can be made. The long-period with respect to the creep–rupture behaviour of GRP rods, i.e. the relation between endurance and stress level, is represented as a straight line on a double algorithmic scale and can also be predicted with the help of the model described. Fig. 21 shows the long-period test results and, as a significant example, those of two short-term tests run with different rise rates, for the material of series E10. This technique is useful if only a few creep–rupture test results are available.

## References


1. L. FRANKE and R. WOLFF, "Glass fiber tendons for prestressed concrete bridges", in 13th IABSE Congress, Helsinki 1988 Session A, Ref. 233.
2. W. ROSEN, "Tensile failure of fibrous composites", in AIAA Aerospace Sciences Meeting, 20–22 January 1964, pp. 64–73.
3. E. OVERBECK, "Zur Bruchfestigkeit und Zeitstandfestigkeit von Glasfasern und unidirektionalen GFK-Stäben", Fortschritt-Berichte VDI, Reihe 5 Grund- und Werkstoffe, no. 127 (1987).
4. C. H. ZWEBEN, *AIAA J.* **6** (1968) 2325.
5. W. WEIBULL, *J. Appl. Mech.* **18** (1951) 324.
6. F. T. PEIRCE, *J. Tex. Inst.* **17** (1926) 355.
7. U. OESTREICH and H. A. AULICH, *Siemens Forsch.-Entwicklung Ber. Bd.* **9** (1980) 123.
8. G. K. SCHMITZ and A. G. METKALFE, *IEC Product Res. Devel.* **5** (1966) 1.
9. A. ZAGANIARIS, "Mechanical reliability of optical fibers", in Congression of optical fibers, Kopenhagen, September 1981, pp. 8–1, 8–4.
10. C. R. KURJAN, "Fiber strength", in Meeting on optical fiber transmission, Washington (1979) p. 10.
11. F. R. JONES and J. W. ROCK, *J. Mater. Sci. Lett.* **2** (1983) 415.
12. S. SAKAGUCHI, *J. Mater. Sci.* **17** (1982) 2878.
13. S. M. WIEDERHORN and L. H. BOLZ, *J. Amer. Ceram. Soc.* **53** (1970).
14. L. FRANKE, "Schadensakkumulation und Restfestigkeit im Licht der Bruchmechanik Fortschritte im konstr. Ingenieurbau" (Rehm–Festschrift, 1984).
15. G. REHM and L. FRANKE, "Kunstharzgebundene Glasfaserstäbe als Bewehrung im Spannbetonbau Schriftenreihe des DAfStb", no. 304 (1979).



*Received 9 May*
*and accepted 20 September 1991*